Organic & Biomolecular Chemistry

Cite this: *Org. Biomol. Chem.*, 2011, **9**, 5787

www.rsc.org/obc

PAPER

Artificial polymeric receptors on the cell surface promote the efficient cellular uptake of quantum dots†

Kenichi Niikura,*[a] Katsuyuki Nambara,[b] Takaharu Okajima,[c] Ryosuke Kamitani,[b] Shin Aoki,[d] Yasutaka Matsuo[a] and Kuniharu Ijiro*[a]

Received 17th March 2011, Accepted 18th May 2011
DOI: 10.1039/c1ob05420a

In our previous paper, secondary-amine appended cationic polymer **1** was used as a scaffold to display artificial receptors on a cell surface (R. Kamitani *et al.*, *ChemBioChem*, 2009, **10**, 230). This polymer can be retained on the cell surface for more than 30 min before being slowly internalized into the cells. In this study, our aim is to achieve the efficient internalization of quantum dots (QDs) into target cells *via* artificial receptors on the polymer. As a receptor molecule, *N*-acetylglucosamine (GlcNAc) moieties were introduced into the polymer, and GlcNAc binding protein-displaying QDs were used as a ligand. We found that ligand-presenting QDs could be internalized effectively into cells *via* polymer-mediated endocytosis, whereas QDs were not internalized into untreated cells. These data suggest that our method based on cell-surface engineering using polymers affords a new approach to the delivery of various poorly permeable nanoparticles into cells.

Introduction

The development of a method for nanoparticle delivery into mammalian cells is of great interest both for the basic insights into cellular function that it can provide, and for its potential applications in biomedicine and diagnostics.[2,3] In particular, quantum dots (QDs) have gained much interest in the past decade for *in vitro* and *in vivo* imaging due to their high quantum yield, size-dependent emission spectra, and resistance to chemical degradation.[4–8] The internalization of QDs into cells is the first and essential step for the labeling of cellular components. In order to accelerate the uptake of nanoparticles by target cells, the nanoparticle surface has been chemically modified with a variety of ligands, recognized by target cells, to induce receptor-mediated endocytosis.[9–12] However, this strategy of nanoparticle delivery is useful only when the target cells overexpress known receptors. Although modification of cationic peptides and polymers with QDs to gain more efficient internalization has been widely explored,[13–16] some problems remain, such as aggregation of QDs and their toxicity.

Instead of natural receptors, the display of artificial receptors on the cell surface offers a valuable approach to inducing cellular uptake of ligand molecules.[17–21] An example of the noncovalent display of receptor molecules on the cell membrane can be found in the work of Peterson and co-workers, who have shown that cholesterol derivatives linked to the binding motif for proteins and drugs act as artificial receptors for efficient drug delivery.[18] These bound molecules are reported to be internalized into cells, and the cholesterol derivatives are returned to the cell membrane within a relatively short period. These cell-surface engineering techniques will increase the number of potential ligand–receptor combinations and make the molecular design of a variety of nanoparticle surfaces possible.

We have reported that the presence of a secondary amine allows polymers to be retained on the cell surface for approximately 30 min before they are slowly internalized into cells.[1] Our aim in this study is to exploit these amine polymers as a scaffold to display artificial receptors on the cell surface, and facilitate intracellular delivery of the ligand-presenting QDs *via* artificial receptor–ligand interactions on the plasma membrane (Fig. 1). Although the polymer coating of cells has been reported by several groups,[21,22] there have been few reports showing that the polymer coating on cells enhances the cellular uptake of nanoparticles. This method has an advantage in that a large number of receptors can be accumulated on the cell surface. The specific binding of ligand molecules to receptors on the polymer is expected to induce the subsequent cellular uptake of the ligands. The receptors clustered along the polymer chain provide multivalent interactions for ligand molecules on the cell membrane, thereby effectively inducing endocytosis of nanoparticles.

[a]*Research Institute for Electronic Science (RIES), Hokkaido, University, Kita21, Nishi10, Kita-Ku, Sapporo, 001-0021, Japan. E-mail: kniikura@poly.es.hokudai.ac.jp*
[b]*Division of Chemistry, Graduate School of Science, Hokkaido University, Japan*
[c]*Graduate School of Information Science and Technology, Hokkaido University, Japan*
[d]*Faculty of Pharmaceutical Sciences, Tokyo University of Science, 2641, Yamazaki, Noda, 278-8510, Japan*
† Electronic supplementary information (ESI) available: Synthetic procedures and identification of compounds. See DOI: 10.1039/c1ob05420a

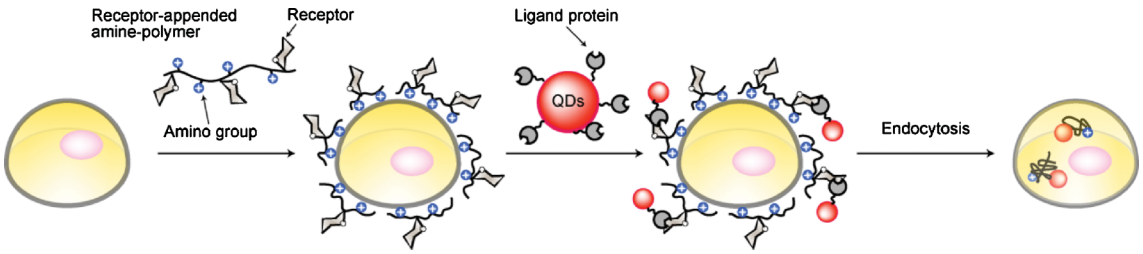

Fig. 1 Schematic presentation of QD internalization mediated by artificial receptor-appended amine polymers.

In our previous paper,[1] we compared retention times on the cell surface of primary- and secondary-amine appended polymers. Herein, we synthesized secondary-, tertiary- and quaternary-amine appended polymers (referred to as *s*-, *t*- and *q*-amine polymers, respectively), and compared the intracellular behavior of these polymers (Scheme 1). GlcNAc, as an artificial receptor, was conjugated to the *s*-amine polymer (referred as GlcNAc polymer), and displayed on the cell surface along the polymer. Two different types of cells, human fibrosarcoma cell line HT1080 cells and human fibroblast cell line TIG1-20 cells, were used to assess nanoparticle delivery by receptor-appended polymer mediation. We demonstrate that QDs coated with GlcNAc-binding protein or wheat germ agglutinin (WGA) as ligand molecules can be taken into HT1080 cells through specific binding to GlcNAc moieties and subsequent artificial receptor-mediated endocytosis.

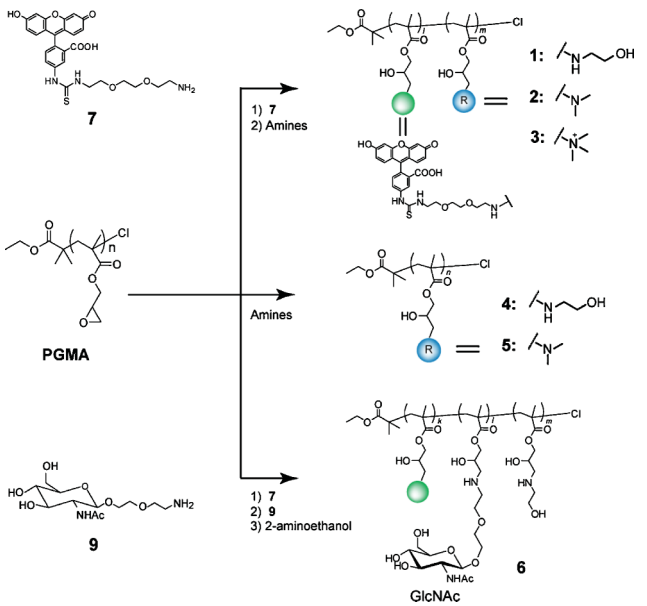

Scheme 1 Chemical structures of various amine-appended polymers **1**–**5** (**1**, **4**: *s*-amine polymer, **2**, **5**: *t*-amine polymer and **3**: *q*-amine polymer) and GlcNAc polymer **6**. Based on M_w value, average polymerization degree (n) of PGMA was calculated as 186.

Results and discussion

A. Differences in cellular uptake between secondary-, tertiary- and quaternary-amine polymers

Synthetic procedures and identification of compounds are described in the ESI†. The amine-appended polymers were synthesized by the modification of poly(glycidylmethacrylate) (PGMA; M_n = *ca.* 25 600, M_w = *ca.* 33 000, M_w/M_n = 1.29). Conjugation of PGMA with ethanolamine and dimethylamine gave the secondary- and tertiary-amine polymers, respectively (Scheme 1). The construction of quaternary ammonium was carried out by the addition of an equimolecular amount of trimethylamine and HCl, according to the previously reported method.[23] For visualization in cells, a small fraction (molecular ratio: 1%) of the epoxide group was simultaneously reacted with amine-derived fluorescein to afford a fluorescent probe to monitor their localization in cells, and with amine-introduced GlcNAc (molecular ratio: 20% to total epoxide groups) to generate GlcNAc polymer **6**.

In this paper, we compare retention times on the cell surface of Fluorescein isothiocyanate isomer I (FITC) labeled *s*-amine polymer **1**, *t*-amine polymer **2** and *q*-amine polymer **3**. These *s*-, *t*- and *q*-amine polymers were incubated separately with HeLa cells for 10 min and, after rinsing with PBS buffer, their localizations were observed using confocal laser scanning microscopy (CLSM) (Fig. 2A). The *q*-amine polymer **3** was rapidly internalized into cells. In contrast, both polymers **1** and **2** were still localized on

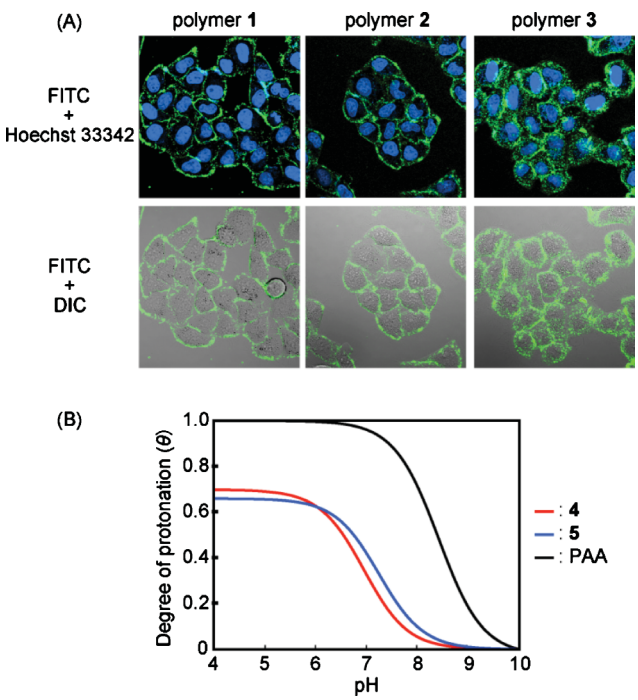

Fig. 2 (A) Fluorescence and differential interference contrast (DIC) images of HeLa cells after incubation with polymers **1**–**3** for 10 min. The nuclei were stained with Hoechst 33342. (B) pH titration curves of polymers **4**, **5** and PAA at 25 °C with I = 0.1 ($NaNO_3$).

the cell surface after incubation for 10 min. Since these polymers were highly water soluble, all cells uniformly interacted with the polymers. Similar results for membrane localization were also obtained in NIH3T3 and Jurkat cells, indicating a general trend in polymer retention (Fig. S1†).

After incubation for 10 min, we investigated the cellular uptake of polymers **1–3** by flow cytometry (Fig. S2†). The *q*-amine polymer **3** was the most readily incorporated into cells among the three polymers, followed by the *s*-amine polymer **1**. This result is consistent with that obtained from CLMS imaging, in which the *q*-amine polymer **3** was seen to be well-internalized into the cells. This indicates that *q*-amine polymer **3** is not suitable for displaying artificial receptors on the plasma membrane because it is rapidly internalized into the cells. From these results, we concluded that *s*-amine polymer **1** would be the most effective cationic polymer for the display of artificial receptors on the cell surface.

We speculated that the differences in the degree of protonation between polymers would be a dominant factor in determining cell-membrane retention. The protonation behavior of the amine moieties in the *s*- and *t*-amine polymers **4**, **5** and primary amine polymer, poly(allylamine) (PAA), as a control, were studied by potentiometric pH titration. The deprotonation process of each hydrochloride-formed polymer was monitored by titration with NaOH. The raw titration data were transformed to give the degree of protonation Θ as a function of pH using the BEST program[24,25] (Fig. 2B), and ionization degrees at pH 7.4 are summarized in Table 1. In the case of PAA, the degree of protonation was found to be 0.91 at pH 7.4, which is in good agreement with the results shown in previous reports.[26] On the other hand, the *s*- and *t*-amine polymers **4** and **5** showed much lower ionization degrees of 0.19 and 0.28 at pH 7.4, respectively. Smits *et al.* reported that the protonation of linear polycations did not proceed completely in an experimentally accessible pH range.[27] This could be due to the electrostatic suppression of the polymer amine groups by neighboring amine cations *via* through-space interactions. The cationic polymers are bound to negatively-charged heparan sulfates on the extracellular domain of syndecans of the cell membrane though electrostatic binding, and this induces syndecan-assembly, thus leading to endocytosis.[28] Since *s*- and *t*-amine polymers **4** and **5** have a lower density of cationic residues than that of PAA and *q*-amine polymer at a neutral pH, the weaker electrostatic interactions between the plasma membrane and polymers would suppress rapid cellular uptake.

B. Localization of the *s*-amine polymer 1 on HT1080 and TIG1-20 cells

We compared the internalization behavior of the *s*-amine polymer **1** using two kinds of cells, HT1080 cells and TIG1-20 cells. In both cells, polymer **1** was localized on the plasma membrane for 10 min (Fig. 3A). However, polymer **1** was internalized into the HT1080 cells within 1 h, whereas it was retained on the plasma membrane of TIG1-20 cells even after 1 h (Fig. 3B). These findings are attributable to differences in endocytic activity between these two cell lines. In order to identify the path of internalization, we examined the effect of temperature on the cellular uptake of polymer **1**. The uptake of polymer **1** was drastically inhibited at 4 °C and, it remained localized on the plasma membrane (Fig. 4). This result demonstrates that endocytosis is the major path of *s*-amine polymer **1** into HT1080 cells.

Table 1 The ionization degree of *s*-amine polymer **4**, *t*-amine polymer **5** and PAA at pH 7.4

Polymer	Ionization degree at pH 7.4
4	0.19
5	0.28
PAA	0.91

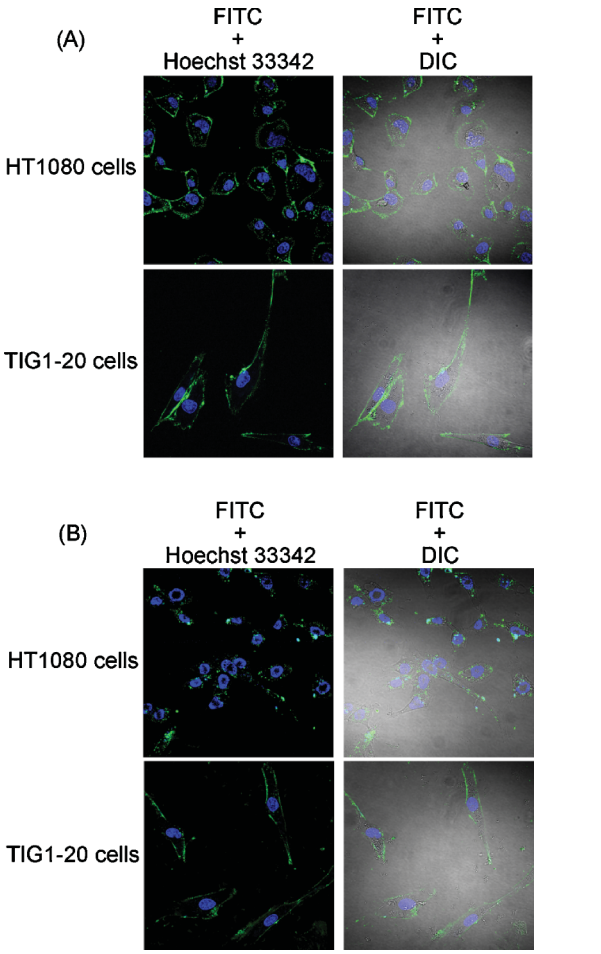

Fig. 3 Fluorescence images of HT1080 and TIG1-20 cells (A) after incubation with *s*-amine polymer **1** for 10 min, (B) after incubation with polymer **1** for 10 min, washed with PBS buffer and subsequent culture for 1 h in serum-free medium at 37 °C. Green; fluorescence (FITC) from polymer **1**, Blue; Hoechst 33342.

C. GlcNAc-mediated cellular uptake of WGA-presenting quantum dots

As a receptor molecule, we appended GlcNAc moieties onto the polymer side chains. We predicted that the GlcNAc moieties of GlcNAc polymer **6** would act as artificial receptors on the plasma membrane as few terminal GlcNAc moieties were present. Similar to the results obtained for polymer **1**, GlcNAc polymer **6** was localized on the plasma membrane of both cells for 10 min and was then slowly internalized into HT1080 cells within 1 h, whereas it was retained on the plasma membrane of TIG1-20 cells even after 1 h (Fig. S3†). These results indicate endocytosis-active cells can

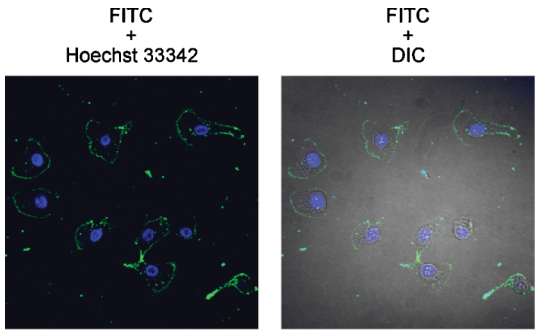

Fig. 4 Fluorescence images of HT1080 cells incubated with polymer **1** for 10 min, washed with PBS buffer and subsequent culture for 1 h in serum-free medium at 4 °C.

easily internalize ligand molecules through the use of polymeric artificial receptors. The total amount of GlcNAc polymer in the HT1080 cells was quantified by flow cytometry analysis. The fluorescence intensity of GlcNAc polymer **6** after incubation for 1 h was approximately 70% of that after just 10 min incubation (Fig. S4†). This result shows that most of the plasma membrane-retained polymers did not dissociate from the plasma membrane but were internalized into the cells.

After adding GlcNAc polymer **6** to cells, the internalization of WGA protein-coated quantum dots (WGA-QDs) through GlcNAc–WGA interactions was monitored by CLSM (Fig. 5). HT1080 and TIG1-20 cells were incubated with GlcNAc polymer **6** for 10 min. After washing the cells with a buffered solution, WGA-QDs were added to the media and incubated for 1 h. In the HT1080 cells, fluorescence from the WGA-QDs was detected inside the cells (Fig. 5A), whereas the WGA-QDs were localized on the cell surface of the TIG1-20 cells (Fig. 5B). As a control, WGA-QDs incubated in the absence of GlcNAc polymer **6** were not internalized into the HT1080 or TIG1-20 cells even after incubation for 1 h (Fig. S5†). These CLSM data were also supported by the results of flow cytometry analysis (Fig. 6). For both HT1080 and TIG1-20 cells, the fluorescence from QDs can be detected only after the treatment of cells with GlcNAc polymers, but not polymer **4**.

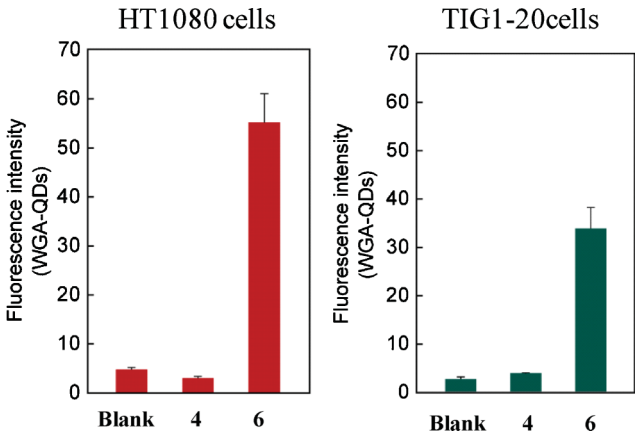

Fig. 6 Flow cytometry analysis of HT1080 and TIG1-20 cells after incubation with WGA-QDs. Cells were pretreated with polymer **4** or **6**. In this experiment, polymer **6** without the appended FITC was used to detect fluorescence from QDs only.

Importantly, it should be noted that the premixture of WGA-QDs and GlcNAc polymer under the same conditions, did not result in cellular uptake (Fig. S6†). This means that the sequential addition of the polymer and WGA-QDs is essential for efficient QD uptakes. Furthermore, the addition of *s*-amine polymer **1** instead of GlcNAc polymer **6** did not result in any significant cellular uptake of WGA-QDs (Fig. S7†), and the addition of an excess of GlcNAc (10 mM) in medium also did not result in any significant cellular uptake of WGA-QDs (Fig. S8†). These data indicate that WGA-QDs were selectively taken into HT1080 cells *via* the plasma membrane-retained polymers displaying artificial GlcNAc receptors, but not nonspecific endocytosis.

Conclusions

In this study, we concluded that the low cationic density of the secondary-amine appended polymers is a key prerequisite for long-term retention on the cell membrane. Monosaccharide GlcNAc moieties were introduced into the polymer as an artificial receptor. The GlcNAc moieties were found to work as a receptor for the

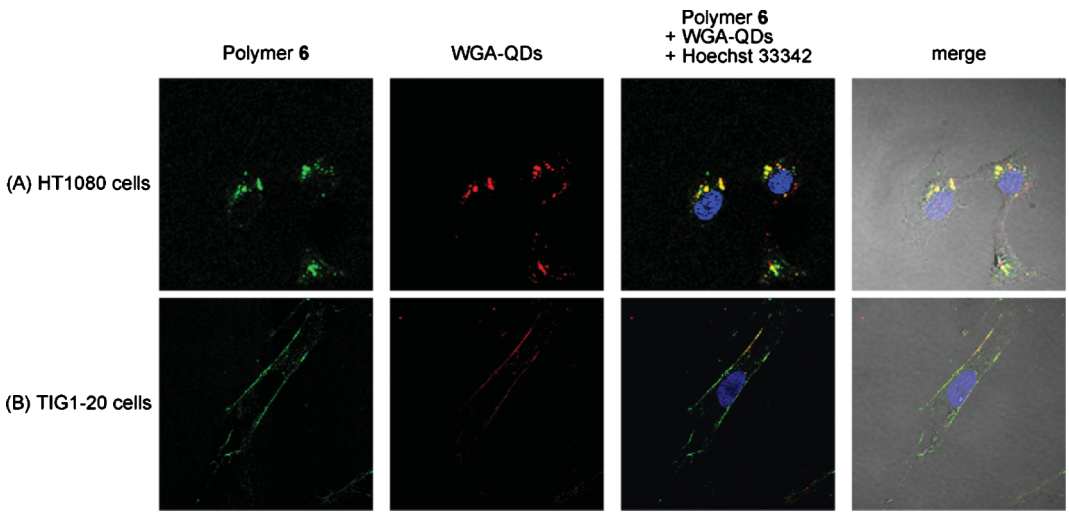

Fig. 5 Fluorescence images of (A) HT1080 and (B) TIG1-20 cells treated with polymer **6** for 10 min and then incubated with WGA-QDs for 1h.

binding and subsequent internalization of ligand-presenting QDs *via* the endocytotic pathway. In contrast, preconjugation of WGA-QDs with the GlcNAc-polymer did not induce the uptake of QDs into cells, indicating that the sequential addition of the polymer and QDs is critical for this approach. Particularly, our approach is useful for cells with high endocytotic activity. The application of this technique would expand the usefulness of cell-surface engineering using artificial ligand–receptor interactions towards cell-specific delivery of nanoparticles into cells.

Experimental

General remarks

Synthetic procedures for the polymers are described in the supplementary material (ESI†). Gel permeation chromatography (GPC) analysis was carried out at 40 °C on the HLC-8220 GPC system (TOSOH, Japan) equipped with a TSK gel Super HM-M column (TOSOH, Japan). Chloroform was used as an eluent at a flow rate of 0.3 mL min^{-1}. Polystyrene standards (Polymer Laboratories, USA) were used to calibrate the GPC system. Confocal laser scanning microscopy (CLSM) employed an Olympus FV300 microscope. Hoechst 33342 was excited with a 405 nm argon ion laser and emitted photons were collected through a 445/15 nm band pass filter. Fluorescein isothiocyanate isomer I (FITC) was excited with a 488 nm argon ion laser and emitted photons were collected through a 510 nm long pass filter. WGA-QDs (Invitrogen, Q12021MP, USA) were excited with a 405 nm laser and emitted photons were collected through a 610 nm long pass filter. All images were processed with Adobe Photoshop 7.0.

Potentiometric pH titration

pH values were determined with a potentiometric automatic titrator (AT-420, KEM, Japan). The electrode system was calibrated with pH 4.01, 6.86, 9.18 buffer solutions and checked by the duplicate theoretical titration curves of 0.10 M HCl aq. solution with 0.10 M NaOH aq. solution at 25 °C and ionic strength (I) = 0.10 M ($NaNO_3$) in high- and low-pH regions. Aqueous solutions (50 mL) of polymers (1.00 mM; amine moiety concentration) with 1.0 equivalent HCl adjusted to 0.10 M with $NaNO_3$ was titrated with 0.1 N NaOH aq. The temperature was maintained at 25.0 ± 0.1 °C. All the solutions were carefully protected from air by a stream of humidified argon. The degree of protonation of the polymers was determined using the program BEST. The total nitrogen content of the samples were determined by elemental analysis and used to normalize the curves to the degree of protonation.

Cell culture

HeLa cells were grown in a monolayer in Dulbecco's modified Eagle medium (DMEM) supplemented with 10% fetal bovine serum (FBS), penicillin (500 units mL^{-1}), and streptomycin (500 μg mL^{-1}). HT1080 cells were grown in DMEM-F12 medium supplemented with 10% FBS, penicillin (500 units mL^{-1}), and streptomycin (500 μg mL^{-1}) and TIG1-20 cells were grown in DMEM-F12 supplemented with 10% FBS. The cultures were kept at 37 °C in a humidified incubator under 5% CO_2.

Incubation of cells with each polymer for CLSM

HeLa (1.0×10^5) cells, HT1080 (1.25×10^5) cells and TIG1-20 (2.0×10^5) cells were seeded in 35 mm glass base dishes separately and cultured for 1 day in the above-mentioned conditions. The cells were washed with PBS (2 × 1.0 mL), then Opti-MEM (2.0 mL) and Hoechst 33342 (2.0 μL) were added. After incubation at 37 °C for 3 min, the cells were washed with PBS (2 × 1.0 mL), and then each polymer, dissolved in Opti-MEM to a compound concentration of 25 μg mL^{-1}, was added to the cells. The cells were incubated in the presence of the polymer at 37 °C for 10 min, washed with PBS (2 × 1.0 mL), and the fluorescence was measured by CLSM.

Inhibition of endocytosis of polymer 1

HT1080 (1.25×10^5) cells were seeded in 35 mm glass base dishes and cultured for 1 day in the above-mentioned conditions. The cells were washed with PBS (2 × 1.0 mL), and *s*-amine polymer **1** dissolved in Opti-MEM was added to the cells. After incubation at 37 °C for 10 min, the cells were washed with PBS (2 × 1.0 mL). The cells were incubated at 4 °C for 1 h, washed with PBS (2 × 1.0 mL), then Opti-MEM (2.0 mL) and Hoechst 33342 (2.0 μL) were added. After washing with PBS (2 × 1.0 mL), the fluorescence was measured by CLSM.

Flow cytometry analysis of each polymer-treated cells

Cells treated with each polymer prepared by the above mentioned method were treated with Trypsin/EDTA (0.05%) at 37 °C for 3 min. After centrifugation, the cells were resuspended in PBS (500 μL) and analyzed by the flow cytometer.

Cellular uptakes of WGA-QDs through GlcNAc polymer 6

HT1080 (1.25×10^5) cells and TIG1-20 (2.0×10^5) cells were seeded in 35 mm glass base dishes separately and cultured for 1 day in the above-mentioned conditions. The cells were washed with PBS (2 × 1.0 mL), and then polymer **6** dissolved in Opti-MEM was added to the cells. After incubation at 37 °C for 10 min, the cells were washed with PBS (2 × 1.0 mL), then WGA-QDs (2 μL in stock solution, 1 μM) were added to the cells. The cells were incubated at 37 °C for 1 h, washed with PBS (2 × 1.0 mL), then Opti-MEM (2.0 mL) and Hoechst 33342 (2.0 μL) were added. After washing with PBS (2 × 1.0 mL), the fluorescence was measured by CLSM.

Acknowledgements

This work was supported by an Industrial Technology Research Grant Program in 2006 from the New Energy and Industrial Technology Development Organization (NEDO) of Japan. The flow cytometry analysis was carried out at the OPEN FACILITY, Hokkaido University, Sousei Hall and HINTS.

Notes and references

1 R. Kamitani, K. Niikura, T. Okajima, Y. Matsuo and K. Ijiro, *ChemBioChem*, 2009, **10**, 230–233.
2 H. Goesmann and C. Feldmann, *Angew. Chem., Int. Ed.*, 2010, **49**, 1362–1395.
3 H. S. Choi, W. Liu, F. Liu, K. Nasr, P. Misra, M. G. Bawendi and J. V. Frangioni, *Nat. Nanotechnol.*, 2009, **5**, 42–47.

4 Z. Medarova, W. Pham, C. Farrar, V. Petkova and A. Moore, *Nat. Med.*, 2007, **13**, 372–377.
5 J. K. Jaiswal, E. R. Goldman, H. Mattoussi and S. M. Simon, *Nat. Methods*, 2004, **1**, 73–78.
6 X. Michalet, F. F. Pinaud, L. A. Bentolila, J. M. Tsay, S. Doose, J. J. Li, G. Sundaresan, A. M. Wu, S. S. Gambhir and S. Weiss, *Science*, 2005, **307**(5709), 538–544.
7 M. J. Bruchez, M. Moronne, P. Gin, S. Weiss and A. P. Alivisatos, *Science*, 1998, **281**, 2013–2016.
8 H. S. Choi, Y. Ashitate, J. H. Lee, S. H. Kim, A. Matsui, N. Insin, M. G Bawendi, M. S. –Behnke, J. V Frangioni and A. Tsuda, *Nat. Biotechnol.*, 2010, **28**, 1300–1303.
9 P. S. Low, W. A. Henne and D. D. Doorneweerd, *Acc. Chem. Res.*, 2008, **41**, 120–129.
10 K. C. Weng, Charles O. Noble, B. P. -Sternberg, F. F. Chen, D. C. Drummond, D. B. Kirpotin, D. Wang, Y. K. Hom, B. Hann and J. W. Park, *Nano Lett.*, 2008, **8**, 2851–2857.
11 V. Sigot, D. J. Arndt-Jovin and T. M. Jovin, *Bioconjugate Chem.*, 2010, **21**(8), 1465–1472.
12 K.-T. Yong, H. Ding, I. Roy, W.-C. Law, E. J. Bergey, A. Maitra and P. N. Prasad, *ACS Nano*, 2009, **3**, 502–510.
13 A. Anas, T. Okuda, N. Kawashima, K. Nakayama, T. Itoh, M. Ishikawa and V. Biju, *ACS Nano*, 2009, **3**, 2419–2429.
14 B. Chen, Q. Liu, Y. Zhang, L. Xu and X. Fang, *Langmuir*, 2008, **24**, 11866–11871.
15 B. C. Lagerholm, M. Wang, L. A. Ernst, D. H. Ly, H. Liu, M. P. Bruchez and A. S. Waggoner, *Nano Lett.*, 2004, **4**, 2019–2022.
16 X. Gao, Y. Cui, R. M Levenson, L. W. K. Chung and S. Nie, *Nat. Biotechnol.*, 2004, **22**, 969–976.
17 J. H. Lee, T. J. Baker, L. K. Mahal, J. Zabner, C. R. Bertozzi, D. F. Wiemer and M. J. Welsh,, *J. Biol. Chem.*, 1999, **274**, 21878–21884.
18 (*a*) B. R. Peterson, *Org. Biomol. Chem.*, 2005, **3**, 3607–3612; (*b*) S. Boonyarattanakalin, S. E. Martin, S. A. Dykstra and B. R. Peterson, *J. Am. Chem. Soc.*, 2004, **126**, 16379–16386; (*c*) Q. Sun, S. Cai and B. R. Peterson, *J. Am. Chem. Soc.*, 2008, **130**, 10064–10065; (*d*) S. L. Hussey and B. R. Peterson, *J. Am. Chem. Soc.*, 2002, **124**, 6265–6273.
19 K. Kato, C. Itoh, T. Yasukouchi and T. Nagamune, *Biotechnol. Prog.*, 2004, **20**, 897–904.
20 R. K. June, K. Gogoi, A. Eguchi, X.-S. Cui and S. F. Dowdy, *J. Am. Chem. Soc.*, 2010, **132**, 10680–10682.
21 J. T. Wilson, V. R. Krishnamurthy, W. Cui, Z. Qu and E. L. Chaiko, *J. Am. Chem. Soc.*, 2009, **131**, 18228–18229.
22 O. Inui, Y. Teramura and H. Iwata, *ACS Appl. Mater. Interfaces*, 2010, **2**, 1514–1520.
23 D.-J. Voorn, W. Ming and A. M. van Herk, *Macromolecules*, 2005, **38**, 3653.
24 A. E. Martell, R. J. Motekaitis, *Determination and Use of Stability Constants*, 2nd edn, VCH, New York, 1992, pp 143–172.
25 (*a*) S. Aoki, M. Zulkefeli, M. Shiro, M. Kohsako, K. Takeda and E. Kimura, *J. Am. Chem. Soc.*, 2005, **127**, 9129–9139; (*b*) S. Aoki, K. Sakurama, N. Matsuo, Y. Yamada, R. Takasawa, S. Tanuma, M. Shiro, K. Takeda and E. Kimura, *Chem.–Eur. J.*, 2006, **12**, 9066–9080; (*c*) Y. Yamada and S. Aoki, *JBIC, J. Biol. Inorg. Chem.*, 2006, **11**, 1007–1023; (*d*) S. Aoki, K. Sakurama, R. Ohshima, N. Matsuo, Y. Yamada, R. Takasawa, S. Tanuma, K. Takeda and E. Kimura, *Inorg. Chem.*, 2008, **47**, 2747–2754; (*e*) S. Aoki, Y. Tomiyama, Y. Kageyama, Y. Yamada, M. Shiro and E. Kimura, *Chem.–Asian J.*, 2009, **4**, 561–573.
26 G. J. M. Koper, R. C. van Duijvenbode, D. D. P. W. Stam, U. Steuerle and M. Borkovec, *Macromolecules*, 2003, **36**, 2500–2507.
27 (*a*) R. G. Smits, G. J. M. Koper and M. Mandel, *J. Phys. Chem.*, 1993, **97**, 5745–5751; (*b*) M. Borkovec, J. Daicic and G. J. M. Koper, *Proc. Natl. Acad. Sci. U. S. A.*, 1997, **94**, 3499–3503.
28 (*a*) I. Kopartz, J.-S. Remy and J.-P. Behr, *J. Gene Med.*, 2004, **6**, 769–776; (*b*) H. Park, Y. Kim, Y. Lim, I. Han and E-. S. Oh, *J. Biol. Chem.*, 2002, **277**, 29730–29736; (*c*) H. Park, I. Han, H. J. Kwon and E.-S. Oh, *Cancer Res.*, 2005, **65**, 9899–9905.

